Information-theoretical analysis of Dirac and nonrelativistic quantum oscillators

I. López-García[1], A. J. Macías[1], S. López-Rosa[2,3] and J. C. Angulo[1,3]

[1]*Departamento de Física Atómica, Molecular y Nuclear, Universidad de Granada, 18071 Granada, Spain*
[2]*Departamento de Física Aplicada II, Universidad de Sevilla, 41004 Sevilla, Spain*
[3]*Instituto Carlos I de Física Teórica y Computacional, Universidad de Granada, 18071 Granada, Spain*

An information-theoretical study of the Dirac oscillator and the usual quantum oscillator is provided, in terms of the respective spatial densities. The comparative analysis is grounded on the values of Shannon entropy, Fisher information, and disequilibrium of both systems in arbitrary states. It is emphasized the dependence of these entropic functionals on the angular frequency and the quantum numbers that characterize the state of the systems, and remarkably also on the different spin-angular momentum coupling schemes. The results are interpreted accordingly with the structural patterns of the corresponding densities, providing information on their spread, uniformity, and disorder.

I. INTRODUCTION

In the last few decades, the study of quantum-mechanical systems by means of different density functionals has increased in interest. Particular attention has been paid to the employment of the powerful tools provided by Information Theory [1], designed to enable a precise description of the system in terms of its representative or characteristic probability distributions.

The applications of those tools include a great diversity of physical and chemical objects, with very different levels of sophistication, ranging from few particle systems [2] to complexly structured molecules [3,4], passing through many-electron atoms and ions [5,6]. Additionally, it is frequent that, for a given system, we can consider different descriptive models according to the level of precision pursued as well as the variables considered.

A complete description of a mono- or many-particle system at a given state, in a time-independent quantum-mechanical framework, requires the knowledge of the corresponding wave function $\Psi(\boldsymbol{r}_1, \ldots, \boldsymbol{r}_n)$, which is the corresponding solution of the eigenvalue equation

$$H\Psi(\boldsymbol{r}_1, \ldots, \boldsymbol{r}_n) = E\Psi(\boldsymbol{r}_1, \ldots, \boldsymbol{r}_n),$$

with H the Hamiltonian operator and E the energy of the considered state. Fortunately, for most purposes regarding a relevant physical description assuming indistinguishability of particles, it is sufficient to deal with the one-particle density [7]

$$\rho(\boldsymbol{r}) \equiv \int |\Psi(\boldsymbol{r}, \boldsymbol{r}_2, \ldots, \boldsymbol{r}_n)|^2 d\boldsymbol{r}_2 \ldots \boldsymbol{r}_n.$$

(no integration is required for monoparticular systems). The density function $\rho(\boldsymbol{r})$ provides a measure of the probability of finding a particle at a given position.

Even more, the grounds of Information Theory guarantees a physically meaningful system description in terms of diverse density functionals, each one quantifying specific features of the system under analysis. In this sense, it is worth mentioning the role played by the Shannon entropy S [8–12], as a measure of the spreading of $\rho(\boldsymbol{r})$ over its whole domain. This quantity was introduced in the framework of Communication Theory, but its name is inspired in the thermodynamical concept of order, quantified by entropy.

Complementary to the Shannon entropy, the disequilibrium D allows to quantify how far from uniformity the density $\rho(\boldsymbol{r})$ is, or equivalently, it can be interpreted as a distance from the equiprobability of finding a particle at arbitrary positions [13,14].

Both Shannon entropy and disequilibrium are usually labeled as global measures, due to their low sensitivity to notable changes in the density at very localized regions. For this reason, it is also interesting to consider additionally the Fisher information I, a local density functional with a higher sensitivity to the abovementioned changes [15–19].

The present work is focused on the information-theoretical analysis of a so well-known system as the harmonic oscillator, considering its quantum-mechanical description for arbitrary angular frequencies. Therefore, it is a monoparticular system, and the probability distributions of the different states are obtained by only squaring the modulus of the respective wave functions.

It should be emphasized that many other studies of the abovementioned characteristics are known, but the majority of them pay attention to the solutions derived from a nonrelativistic Hamiltonian. Many of those studies consider some other features of quantum oscillators, including, e.g., statistical correlations [20–22], confinement [23–28], uncertainty [29] or time dependence [28].

Not only the quantum oscillator, but some other quantum-mechanical systems at different levels of sophistication, have been analyzed from an information-theoretic perspective, with the aim of quantifying relativistic effects on the descriptive distributions [30,31]. At times, the functionals employed are interpreted as complexity measures, a notion briefly discussed in Sec. III. Such is the case of atomic systems at the ground

state [30], considering both relativistic and nonrelativistic complexity measures in conjugate spaces, for which the main conclusions are derived from the dependence of such comparative indexes on the nuclear charge and shell structure of the multielectronic systems.

In this sense, it is worth remarking that the Dirac oscillator, described within a relativistic framework, belongs to the class of the few relativistic systems that admits a fully analytical description (as also occurs with hydrogen [31–33]).

Of course, the oscillator solutions are modified, to a greater or lesser extent, depending on whether or not the relativistic description is taken into account. This means that the density functions arising from the relativistic Dirac oscillator differ from the nonrelativistic ones.

The transition from the ordinary to the Dirac oscillator makes analytical treatment evolve in difficulty, mainly due to the need to handle Dirac matrices in the relativistic case. The corresponding differential equations give rise to solutions composed by a couple of kets, each with its own radial and angular factors. This is contrast with the ordinary harmonic oscillator, which wave functions are fully factorized in a unique radial part and a unique angular one, thus facilitating its analytical treatment at different levels.

Additionally, in obtaining the Dirac wave functions, it is necessary to distinguish the different couplings between orbital angular momentum and spin. In fact, this is an essential point when considering the closeness of the Dirac solutions to the nonrelativistic ones, as will be quantified in next sections by employing a diversity of information-theoretical tools.

The main aim of this work is to analyze the differences just pointed out, among the relativistic and non-relativistic probability distributions, for different states and frequencies of the oscillator. In doing so, a comparative study on the respective values of Shannon entropy, disequilibrium and Fisher information is carried out.

In Sec. II, a brief description of the quantum harmonic oscillator and its relativistic counterpart is provided, paying attention to the analytical expressions of the eigenvalues, eigenfunctions, and probability distributions. Then, in Sec. III, the explicit definitions of the density functionals employed are given, together with their information-theoretical meanings and their main properties as well. The resulting numerical values of distributions and functionals are discussed in Sec. IV, interpreting them in physical terms. Finally, some conclusions are derived, and different emerging open problems are pointed out as well.

II. QUANTUM HARMONIC OSCILLATOR AND DIRAC OSCILLATOR DENSITIES

This section is devoted to the theoretical grounds of the systems under study, namely the Dirac oscillator (DO) (thus in a relativistic framework) and its nonrelativistic counterpart (which will be referred to simply as the quantum harmonic oscillator (QHO).

Focusing on the spherically symmetric distributions analyzed in this paper, we highlight that the Dirac oscillator belongs to the class of the few relativistic systems that admits a fully analytical description [34–37].

The Dirac wave function in coordinate representation is given by the solution of the Dirac matricial differential equation of a particle moving in an oscillatory potential ($\hbar = c = 1$ are set):

$$(\boldsymbol{\alpha} \cdot (\mathbf{p} - im_0\omega\beta\mathbf{r}) + m_0\beta)|\Psi\rangle = -i\frac{\partial}{\partial t}|\Psi\rangle, \quad (1)$$

where $\boldsymbol{\alpha}$ and β are the 4×4 Dirac matrices ($\boldsymbol{\alpha}$ defined in terms of the Pauli matrices $\boldsymbol{\sigma}$) [38], ω is the oscillator frequency, and m_0 the mass of the particle. The spinorial eigenfunctions are represented as

$$|\Psi\rangle = \begin{pmatrix} |\phi\rangle \\ |\chi\rangle \end{pmatrix} \exp(-iEt), \quad (2)$$

yielding two coupled equations on $|\phi\rangle$ and $|\chi\rangle$.

These two solutions take into account the set of commuting operators $\{\mathcal{H}, \boldsymbol{J}^2, J_z, \boldsymbol{L}^2\}$, where $\mathcal{H} = \frac{\mathbf{p}^2}{2m_0} + \frac{1}{2}m_0\omega^2\mathbf{r}^2$ [which is not the Hamiltonian of the system, given by the left-hand-side of Eq. (1)] and $\boldsymbol{J} = \boldsymbol{L} + \frac{1}{2}\boldsymbol{\sigma}$, with $\boldsymbol{L}$ being the angular momentum, and $\boldsymbol{\sigma}$ being the Pauli matrices [34]. It is necessary to remark that $|\phi\rangle$ is an eigenvector of $\boldsymbol{L}^2$ with eigenvalue $l(l+1)$ and $|\chi\rangle$ with a different one, $l'(l'+1)$ as described below.

This set of commuting operators leads to the description of the system in terms of the quantum numbers n, j, m. In addition, the spin-angular momentum coupling will be taken into account by means of a new parameter ϵ, defined in terms of the parity $(-1)^l$ as

$$\epsilon = \begin{cases} +1 & \text{if parity is } (-1)^{j+\frac{1}{2}}, \\ -1 & \text{if parity is } (-1)^{j-\frac{1}{2}}. \end{cases} \quad (3)$$

In order to distinguish the above cases when analyzing the DO, the notations DO+ and DO− will be considered for the respective values $\epsilon = \pm 1$.

In what follows, we discuss all the results in terms of $\{N, l, \omega, \epsilon\}$, with N the *radial quantum number* given by $n = 2N + l$, and with $l = j + \frac{\epsilon}{2}$. This description is convenient due to the wave-function expressions (both Schrödinger and Dirac) and the fact that we will only analyze the radial part of the systems.

The energy included in the eigenvalues corresponding to $|\phi\rangle$ and $|\chi\rangle$ becomes expressed as [34]

$$E_{nl} = \pm m_0 \left\{ 1 + 2\omega m_0^{-1} \left[n + 1 + \epsilon \left(l - \frac{\epsilon}{2} + \frac{1}{2} \right) \right] \right\}^{\frac{1}{2}}. \quad (4)$$

For the sake of simplicity in notation, at times we will refer to the above energy as E.

The normalization conditions

$$\langle \phi|\phi \rangle = \frac{1}{2}\left(1 + \frac{m_0}{E} \right), \quad (5)$$

$$\langle \chi|\chi \rangle = \frac{1}{2}\left(1 - \frac{m_0}{E} \right), \quad (6)$$

lead to the following Dirac ket (for the explicit calculation, see Ref. [34]) in the coordinate representation, for $j = l \pm \frac{1}{2}$:

$$\Psi^{\pm}(\mathbf{r}, t) = \begin{pmatrix} iF_{Nl}(r)V_{jml}^{\pm}(\Omega) \\ G_{N'l'}(r)V_{jml'}^{\mp}(\Omega) \end{pmatrix} \exp(-iEt) \quad (7)$$

with Ω denoting the three-dimensional solid angle. Both rows are factorized into radial and angular parts. The angular functions $V_{jml}^{\pm}(\Omega)$ are the spinor spherical harmonics, each one expressed in terms of the two spherical harmonics $Y_{l,m\pm 1/2}(\Omega)$.

The so-called large (F) and small (G) components of the wave function are given by

$$F_{Nl}(r) = \left[\frac{1}{2}\left(1 + \frac{m_0}{E}\right)\right]^{1/2} C_{Nl}R_{Nl}(r), \qquad (8)$$

$$G_{N'l'}(r) = \text{sgn}(E)\left[\frac{1}{2}\left(1 - \frac{m_0}{E}\right)\right]^{1/2} C_{N'l'}R_{N'l'}(r) \qquad (9)$$

with

$$R_{Nl}(r) = {}_1F_1\left(-N; l + \frac{3}{2}; m_0\omega r^2\right)(m_0\omega r^2)^{l/2}$$

$$\times \exp\left(-\frac{1}{2}m_0\omega r^2\right), \qquad (10)$$

$$C_{Nl} = (m_0\omega)^{3/4}\epsilon^N\left[\frac{2^{l-N+2}(2N+2l+1)!!}{\pi^{1/2}N!\{(2l+1)!!\}^2}\right]^{1/2}. \qquad (11)$$

We have introduced the new definitions $l' = l - \epsilon$, as well as $N' = N - \frac{1}{2}(1 - \epsilon)$, restricted to $N, N' \in \mathbb{N}$ by the finiteness of the sum defining the Kummer's function ${}_1F_1(x; y; z)$. The energy E in the above expressions, given by Eq. (4), becomes now expressed as

$$E_{Nl} = \pm m_0\left\{1 + [4N + (\epsilon+1)(2l+1)]m_0^{-1}\omega\right\}^{\frac{1}{2}}, \qquad (12)$$

in terms of the quantum numbers N, l.

The global normalization of the wave function is given by $\int |\Psi(\mathbf{r})|^2 d\mathbf{r} \equiv \int \rho(\mathbf{r})d\mathbf{r} = 1$, with $\rho(\mathbf{r})$ being the probability density of finding the particle somewhere in the space. The factorization of $\Psi(\mathbf{r})$ into radial and angular parts in Eq. (7) leads to respective independent normalizations, giving rise to the condition

$$\int_0^\infty r^2[F_{Nl}^2(r) + G_{N'l'}^2(r)]dr \equiv \int_0^\infty 4\pi r^2 \rho(r)dr = 1, \quad (13)$$

where the function $\rho(r)$ does not include the angular factors of the wave function. In fact, $\rho(r)$ is the spherical average of $\rho(\mathbf{r})$, so that the function $4\pi r^2 \rho(r)$ constitutes the probability density of finding the particle at a given distance from the origin.

The nonrelativistic limit is well-known and is given by the coordinate representation of the wave function [38]:

$$\psi_{Nlm}(\mathbf{r}) = \left[\frac{2N!\nu^{l+\frac{3}{2}}}{\Gamma\left(N+l+\frac{3}{2}\right)}\right]^{1/2} r^l e^{-\frac{\nu}{2}r^2} L_N^{l+\frac{1}{2}}(\nu r^2)Y_{lm}(\Omega), \qquad (14)$$

with $\nu = m_0\omega$, $L_N^{l+\frac{1}{2}}$ are the generalized Laguerre polynomials and $Y_{lm}(\Omega)$ the spherical harmonics (m the eigenvalue of the operator L_z). The energy of a given state is

$$E_{nlm} = \omega\left(n + \frac{3}{2}\right), \qquad (15)$$

with $n = 2N + l$, and $N \in \mathbb{N}$ determines the degree of the Laguerre polynomial. And similarly to the Dirac case, the nonrelativistic distributions $\rho(\mathbf{r})$ and $\rho(r)$ are defined from $|\psi_{Nlm}|^2$ [39,40].

Let us mention the similar expressions holding in the conjugate (momentum) space, for both the wave function $\tilde{\Psi}(\mathbf{p}, t)$ and the one-particle density $\gamma(\mathbf{p})$, due to the interconnection between the gaussian-like functions Ψ and $\tilde{\Psi}$ by means of a Fourier transform. In fact, it is easy to prove that

$$\gamma(\mathbf{p}) = \nu^{-3}\rho(\mathbf{p}/\nu). \qquad (16)$$

III. INFORMATION THEORETIC MEASURES

The aim of this work is to study the different states of the relativistic and nonrelativistic quantum oscillators, in terms of specific information-theoretic functionals of the respective spatial distributions.

The spread of the probability density, $\rho(\mathbf{r})$, that characterizes the state of quantum-mechanical mono- or multielectronic systems (e.g., atoms, molecules) in position space, is related to their physicochemical properties [41]. There exists different measures able to quantify and grasp this spreading, some of them arise within the framework of Information Theory [7,17,42–46]. Beyond the well-known standard deviation or its square, i.e., the variance, the most widely used is the Shannon entropy S, which definition is given in terms of a logarithmic functional [8]:

$$S[\rho] = -\int \rho(\mathbf{r})\ln\rho(\mathbf{r})d\mathbf{r}. \qquad (17)$$

This measure quantifies the total delocalization of the probability density over its whole domain. The value of $S[\rho]$ is maximal when knowledge of $\rho(\mathbf{r})$ is minimal, and thus becoming delocalized. It is worth mentioning that the Shannon entropy is not an *a priori* bounded magnitude, so it can reach negative values. In order to avoid this, the exponential Shannon entropy is often used:

$$L[\rho] = e^{S[\rho]}. \qquad (18)$$

This quantity is also known as the Shannon length, because it has the same dimensions as the independent variable considered, as well as the standard deviation, one of the most widely used uncertainty measures.

The disequilibrium [47], self-similarity [48] or information energy [49], D, quantifies the departure from uniformity (equiprobability) of the density function. It is defined as a power functional [47,49], given by

$$D[\rho] = \int \rho^2(\mathbf{r})d\mathbf{r}. \qquad (19)$$

This expression arises from its discrete and finite counterpart. It is initially provided by summing the squares $(p_i - 1/N)^2$ of the differences between each probability p_i and the respective term $1/N$ for equiprobability. The transition to the continuous case (implying $N \to \infty$) gives rise to Eq. (19).

Disequilibrium D, together with the Shannon entropy S, are the essential ingredients in defining the pioneering measure of complexity C for arbitrary distributions [47]. This concept refers to the departure, in some way, from the situations of extreme order/disorder. The initial definition of López-Mancini-Calbet (LMC) complexity was later modified [50], by replacing the Shannon entropy S by the Shannon length L, as $C_{LMC} = DL$. This expression complies with different desirable properties for any complexity measure.

Both measures defined above, namely Shannon entropy and disequilibrium, have a global character, i.e., they are determined by the behavior of the probability density over its whole domain. In contrast to these two quantities, the Fisher information I defined below is a local measure because its definition constitutes a functional enclosing not only the own density, but its gradient as well [15,18]:

$$I[\rho] = \int \frac{|\boldsymbol{\nabla}\rho(\mathbf{r})|^2}{\rho(\mathbf{r})} d\mathbf{r}. \tag{20}$$

This quantity is very sensitive to the strong changes on the distribution over small-sized regions. It quantifies the gradient content of the distribution hence revealing the irregularities of the density and providing a quantitative estimation of its fluctuations.

It is worth remarking that the Fisher information I is enclosed in the definition of complexity measures after the pioneering LMC one. Such is the case of the productlike Fisher-Shannon (FS) [51] and Cramér-Rao (CR) [1] complexities, combining I with a global functional (Shannon entropy and variance, respectively).

Let us focus for a moment on the analysis of the above functionals $\{S, D, I\}$ for quantifying the respective aspects of the different states (as characterized by N, l quantum numbers) of the QHO, and those of both coupling versions of the Dirac oscillator (DO+ and DO−, corresponding to $\epsilon = \pm 1$, respectively). The actual work could also serve, in the near future, for an in-depth analysis of the LMC, FS, and CR complexities.

It is worth noting that, in the analytical expression of the QHO function $\rho_{Nl}(\mathbf{r})$, the angular frequency ω appears systematically and exclusively via the term ωr^2 (apart from the normalization constant). As for any arbitrary normalized-to-unity function with a dependence $f(\omega r^2)$, it is guaranteed the proportionality of each of the above functionals L, D, I of $\rho_{Nl}(\mathbf{r})$ to some power ω^λ of the angular frequency, the power λ being independent of $\rho_{Nl}(\mathbf{r})$.

The above property is due to the fact that, varying the value of the parameter ω for such a function $f(\omega r^2)$, preserving normalization, is equivalent to carry out a scale transformation. So, the previous comment means that the quotient of any of the above functionals and its corresponding power ω^λ is invariant under scale trasnformations.

In fact, this is true for the so-called Rényi entropies $R_\alpha[\rho]$ of order α, namely [52]

$$R_\alpha[\rho] = \frac{1}{1-\alpha} \ln \int \rho^\alpha(\mathbf{r}) d\mathbf{r}, \tag{21}$$

for arbitrary α whenever $R_\alpha[\rho]$ be well defined. In a similar fashion as for the Shannon length $L[\rho]$, the Rényi lengths are defined as $L_\alpha[\rho] = \exp\{R_\alpha[\rho]\}$.

Some interesting particular cases correspond to the values $\alpha = 1$ and $\alpha = 2$, providing, respectively, the Shannon entropy and the disequilibrium:

$$S[\rho] = R_1[\rho]; \quad D[\rho] = \exp\{-R_2[\rho]\}. \tag{22}$$

Emphasizing the ω dependence for the $f_\omega(r^2) \equiv f(\omega r^2)$ distributions, the Rényi-like scaling property (for arbitrary α) reads as $R_\alpha[f_\omega] = R_\alpha[f_1] - \frac{3}{2} \ln \omega$. In other words, there exists a linear dependence among any Rényi entropy $R_\alpha[f_\omega]$

and the logarithm $\ln \omega$ of the scaling parameter (particularly the angular frequency), with slope $-3/2$. Equivalently in terms of Rényi lengths, it is found the proportionality relation $L_\alpha[f_\omega] = C\omega^{-3/2}$, with C independent of ω. Notice the additional implication that any quotient $L_\alpha[f_\omega]/L_\beta[f_\omega]$ is ω-independent.

Regarding the particular cases we are focusing on, the linear relations among $S[\rho]$ and $\ln \omega$ with slope $-3/2$ on one hand, and $\ln D[\rho]$ and $\ln \omega$ with slope $3/2$ on the other, have been determined.

With similar arguments to those regarding Shannon and Rényi entropies, a proportionality between the Fisher information $I[f_\omega]$ and the angular frequency ω is derived. In fact, the power of the scaling parameter is the unity for the Fisher functional, so that the corresponding relation reads now as $I[f_\omega] = C\omega$, for some independent-of-ω factor C. In other words, there exists a linear dependence between the logarithms of I and ω.

In what concerns the DO and the corresponding distributions $\rho_{Nl\pm}(\mathbf{r})$, let us remember that they are built up from the large and small components, $F_{Nl}(r)$ and $G_{N'l'}(r)$ in Eqs. (8) and (9), respectively. In fact, the radial factor $\rho_{Nl\pm}(r)$ is obtained from the sum of their squares.

Regarding the above scaling properties of the functionals $\{L, D, I\}$, it is worth remarking that they would hold for each separate term $F_{Nl}^2(r)$ and $G_{N'l'}^2(r)$ of the sum giving rise to the density, if both would be properly normalized (i.e., with ω-independent respective norms). However, the scale invariance does **not** apply to the whole density $\rho_{Nl\pm}(\mathbf{r})$. The reason is that the aforementioned norms of the large/small components, in spite of summing unity as shown in Eqs. (5) and (6), depend on ω separately in different ways.

More precisely, the two norms are expressed in terms of the energy E as $\frac{1}{2}(1 \pm \frac{1}{E})$, and the energy depends on the angular frequency as given by Eq. (4).

Anyway both norms become identical (with value $1/2$) in the limit $E \to \infty$, reached (for a given state) as the frequency ω increases (and also for fixed ω as N increases). Consequently, a linearization should be expected of the dependence on $\ln \omega$ of the different functionals for arbitrary states (as in the QHO case) as far as ω becomes larger.

The above comments on the functionals, together with Eq. (16) for momentum space densities, allow us to straightforwardly extend the conclusions obtained from the numerical study in position space to the momentum space. This is done by only replacing the angular frequency ω by its inverse $1/\omega$. Thus, only distributions in $\mathbf{r}$ space are considered in what follows.

IV. NUMERICAL RESULTS

In this section, structural patterns of the oscillator densities are described, accordingly with the values of the characteristic quantum numbers (N, l, ϵ) for a given state. This includes, e.g., concentration of the density in specific regions (particularly around the origin), or number and heights of local extrema.

Next, those patterns are interpreted in terms of information-theoretical functionals. As described in Sec. III, a diversity of density functionals are defined with the aim

of quantifying different structural features of the probability distributions, such as, e.g. spreading, uniformity or disorder.

The above is done for the QHO, and the Dirac oscillator (DO±), thus including or not a relativistic description of the system. For the sake of simplicity, a reference mass $m_0 = 1$ will be considered throughout the numerical section. Consequently, atomic units (a.u.) are used in what follows.

For the numerical analysis, only the radial parts of the distributions $\rho(\mathbf{r})$ will be considered. In other words, we will refer to the density or distribution, in fact being its spherical average $\rho(r)$, which depends only on the radial variable r.

A. Structural patterns of the density

Due to the presence of Laguerre polynomials in the expressions of the Schrödinger and Dirac wave functions, and consequently on those of the spatial densities, we expect an increasingly rich structure with the radial quantum number N (i.e., the degree of the polynomial). Additionally the orbital angular momentum l modifies the coefficients of the polynomials and their weight function as well.

The following structural changes have been observed when varying N, l and ω:

(1) The joint analysis of plots in Fig. 1 reveals the just mentioned changes as the value of N increases. On one hand, the probability density spreads along regions of space further away from the origin, with significantly non-null values. On the other, the height of the main maximum, which is the closest one to the origin, increases as N increases. In the specific cases of the DO+ and DO− systems, it is observed that the first few minima, particularly those of DO−, have a greater height than the furthest ones (which are roughly zero). Thus, increasing N entails an increase of the number of minima with values far from 0 in the DO± cases. Let us remind the reader that all minima of QHO are exactly zero.

(2) Figure 2 displays a lowering of the height of all maxima for increasing l, equalizing their relative height (i.e., leading to more equiprobable probability distributions), and shifting them away from the origin. In addition, heights of all minima become reduced for DO− and particularly for DO+, whose density becomes very similar to that of QHO for higher $l's$.

(3) A deeper study, not displayed in the above figures, reveals that as ω increases for any of the three systems, regions with probability significantly higher than zero tend to concentrate towards the origin.

In what follows, regarding the analysis of the density functionals, a fixed value of angular frequency ω is considered, taking into account the well-known dependency of the different functionals on it, at least excepting extremely low ω values for DO±.

B. Shannon entropy

Let us firstly focus on the Shannon entropy $S[\rho]$ of the systems we are dealing with. As emphasized in previous sections, the functional $S[\rho]$ constitutes a measure of spatial delocalization of the distribution $\rho(r)$. It is in this sense that the next comparative analysis among the Shannon entropies of the different systems and/or states (as characterized by appro-
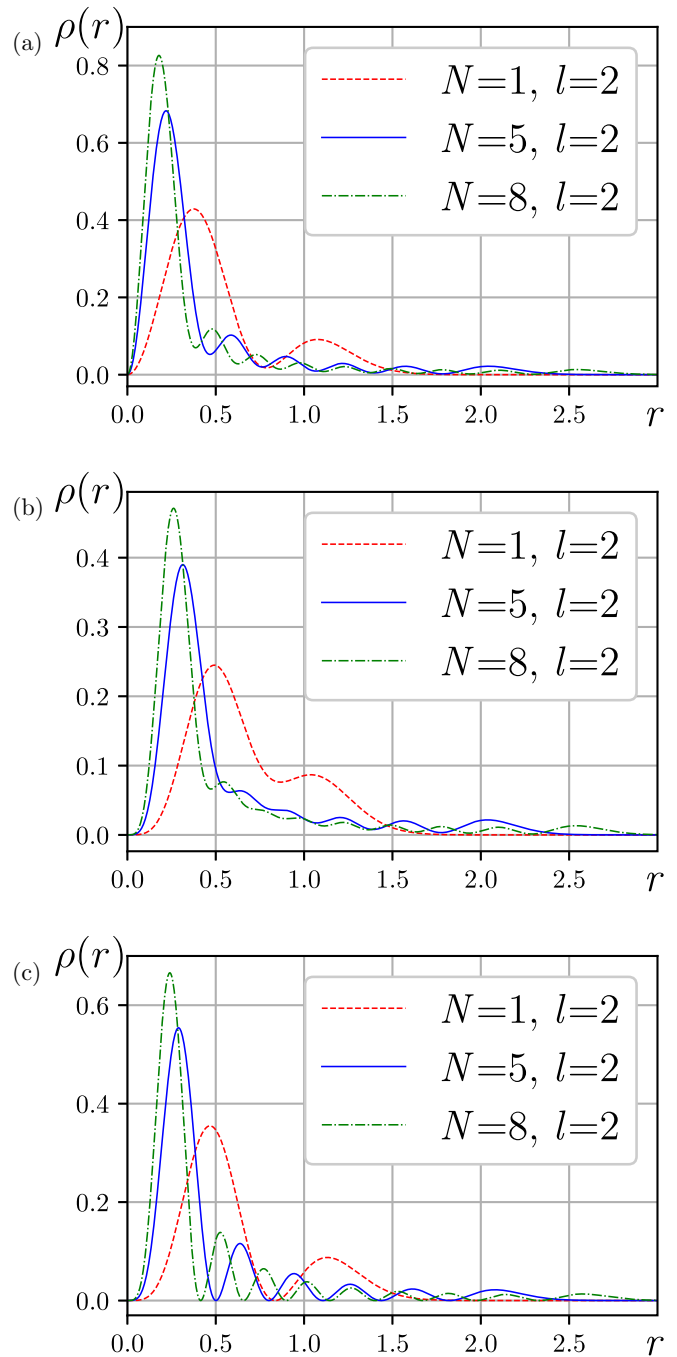

FIG. 1. Density $\rho(r)$ for angular frequency $\omega = 5$, with fixed $l = 2$ and values $\{N = 1, 5, 8\}$, of systems (a) DO+, (b) DO−, and (c) QHO. Atomic units (a.u.) are used.

priate quantum numbers) provides an eventual interpretation of structural patterns of the density in terms of relativistic effects and/or excitation levels.

A first look at Fig. 3, displaying $S[\rho]$ as a function of the radial quantum number N, clearly reveals the increasing monotonicity of all curves. Each curve corresponds to (i) one of the three systems, and (ii) a fixed value of the orbital angular momentum, particularly $l = 1, 12, 20$.

The curves appear to be grouped accordingly with the l value, in sets of three lines, perfectly ordered along the whole range $N = 0 - 15$, with increasing height as l increases. On
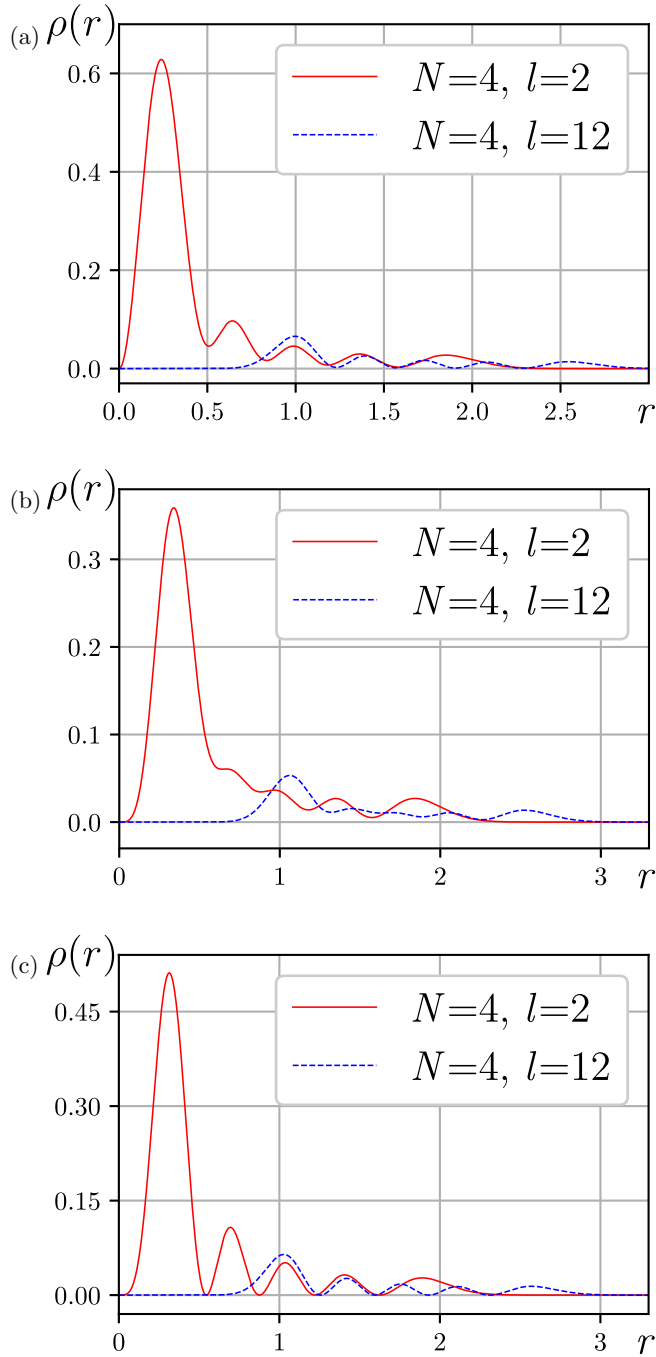
FIG. 2. Density $\rho(r)$ for angular frequency $\omega = 5$, with fixed $N = 4$ and values $\{l = 2, 12\}$, of systems (a) DO+, (b) DO−, and (c) QHO. Atomic units (a.u.) are used.

the other hand, within a given set of curves (i.e., for fixed l), the ordering of the three curves for the corresponding systems (QHO and DO±) is almost systematic, with very few exceptions. This is revealed by the existence of some line crossings among QHO and DO+: from $N = 2 - 3$ (with $l = 1$), and from $N = 1 - 2$ (with $l = 12, 20$). In other words: most usually the Shannon entropy of QHO is lower than that of DO+ (i.e., the Dirac one is more spread out), with the exceptions $N = 0, 1$, and also $N = 2$ for $l = 1$. Systematically, entropy of DO+ is below entropy of DO−.

Some of the above observations are interpreted accordingly to the structural features of the densities plotted in Figs. 3 and 4, as follows:

(1) Minima of the DO− density are larger than those of QHO and DO+. As normalization is preserved, this leads to a higher delocalization of the particle and, consequently, to a higher entropy $S[\rho]$ for arbitrary values of N and l.

(2) As l increases the entropy increases, so obtaining more equiprobable distributions. For high values of l, the DO+ and QHO entropies converge one to each other, due to the structural similarity of their densities.

(3) As N increases, the uncertainty in the position of the particle becomes larger, and therefore the entropy increases. This is especially relevant for the DO± systems, with higher entropies as compared to that of the QHO system for large N.

(4) Crossovers (see Fig. 3) between curves of DO+ and QHO entropy are observed for low N and l, as mentioned above. For illustration, let us notice that $S_{DO+} < S_{QHO}$ for $N < 2$ and arbitrary l. Analyzing the respective densities in Fig. 1, DO+ displays a high maximum close to the origin, giving rise to a region where the DO+ distribution is more localized as compared to the QHO one.

(5) Increasing ω compresses the density towards the origin, for all three systems. The accumulation of the distribution around a point reduces the size of the region most likely to find the particle, so that the particle becomes more localized and therefore the entropy tends to decrease with increasing ω.

An in-depth numerical analysis of the Shannon entropies displayed in Fig. 3, regarding the dependency on the radial quantum number N, reveals a powerlike behavior as $S \sim N^a$. The accuracy of the fits slightly depends on the system considered (QHO, DO+ and DO−), and on the orbital angular momentum l. In Table I, the powers of the fitted curves are provided for a diversity of l values, together with the respective correlation coefficients.

Some comments are in order:

(1) For all the three systems, the power a decreases as l increases, roughly from 0.3 ($l = 1$) to 0.1 ($l = 20$). This means that the increasing trend of $S[\rho]$ with N becomes softer for larger angular momenta.

(2) For a given l, the three corresponding a values are similar, the more the higher l is. Nevertheless, the highest power is displayed systematically by the DO+ system, while those of QHO and DO− are much closer to each other. Thus, the entropy of DO+ increases with N faster than those of the other systems.

(3) All correlation coefficients are above 0.98, with higher accuracies for lower l values.

(4) The value $N = 0$ has not been included for the fittings, based on a log-log regression.

For fixed N, the Shannon entropy also displays an increasing behavior with the orbital angular momentum l, as shown in Fig. 4 for the illustrative cases $N = 1, 4, 15$. Again a powerlike dependence is found, within the whole l range here considered for low N's, and for large l at least as N becomes larger. Some details are given below:

(1) Respective fittings $S \sim A\, l^a$ provide, roughly for the three systems, $2.1l^{0.22}$ ($N = 1$), $2.9l^{0.16}$ ($N = 4$ within the range $l = 5 - 25$) and $4.2l^{0.095}$ ($N = 15$ for $l = 10 - 25$). All correlation coefficients are above 0.99.
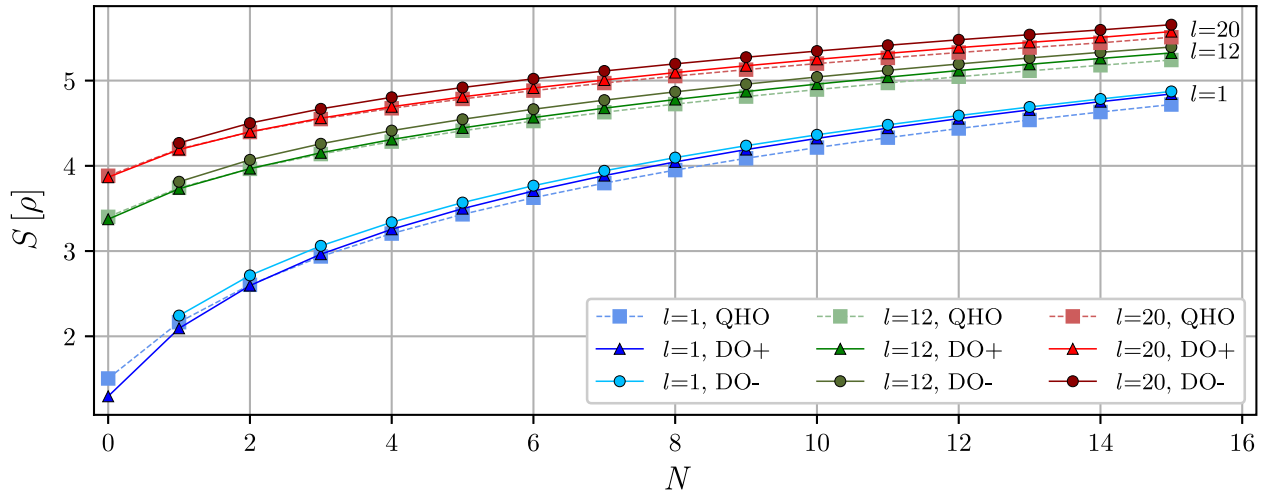
FIG. 3. Shannon entropy $S[\rho]$ as a function of the radial quantum number N, for systems DO$\pm$ and QHO with $\omega = 5$. Atomic units (a.u.) are used.

(2) Consequently, the increase of entropy with l becomes softer as N increases. On the other hand, the fitted value at $l = 1$ varies (roughly) as $2.1, 2.9, 4.2$ (for $N = 1, 4, 15$, respectively). This is true for QHO, DO+, and DO−.

(3) There is not a systematic ordering, for a given N, of fitting powers for the three systems. As indicated above, the three values are similar. However, let us remark that the lowest power corresponds to DO− in the $N = 1, 4$ cases, but to DO+ for $N = 15$.

In Ref. [39], a thorough information-theoretic analysis on the d-dimensional quantum harmonic oscillator is provided, considering also arbitrary energetic states. The main difference, as compared to the present work, is that only the nonrelativistic solutions are considered, but in both conjugate spaces and including the angular part. The study is limited to Shannon entropy, paying attention to its dependence on the state quantum numbers. The numerical analysis regards the three-dimensional case with fixed frequency. The main conclusions in Ref. [39] are: (i) the Shannon entropy displays an increasing trend with the principal quantum number n, and (ii) the curves of Shannon entropies in position and momentum spaces are roughly identical (apart from a shifting constant). Such conclusions are in agreement with those here derived. Additional results are provided regarding the angular factor (with dependence on $|m|$ as well).

C. Disequilibrium

The analysis of disequilibrium $D[\rho]$ for the harmonic oscillators in terms of the quantum numbers (N, l) allows us to quantify the departure from uniformity/equiprobability of the respective distributions $\rho(r)$. One of the aims is to interpret the disequilibrium values accordingly with the structural properties of the corresponding densities, in a similar fashion as previously done with Shannon entropy. Let us here remind the reader of the global character of both magnitudes $D[\rho]$ and $S[\rho]$.

In Fig. 5, the disequilibrium $D[\rho]$ is displayed for fixed values of the orbital angular momentum l, and varying the radial
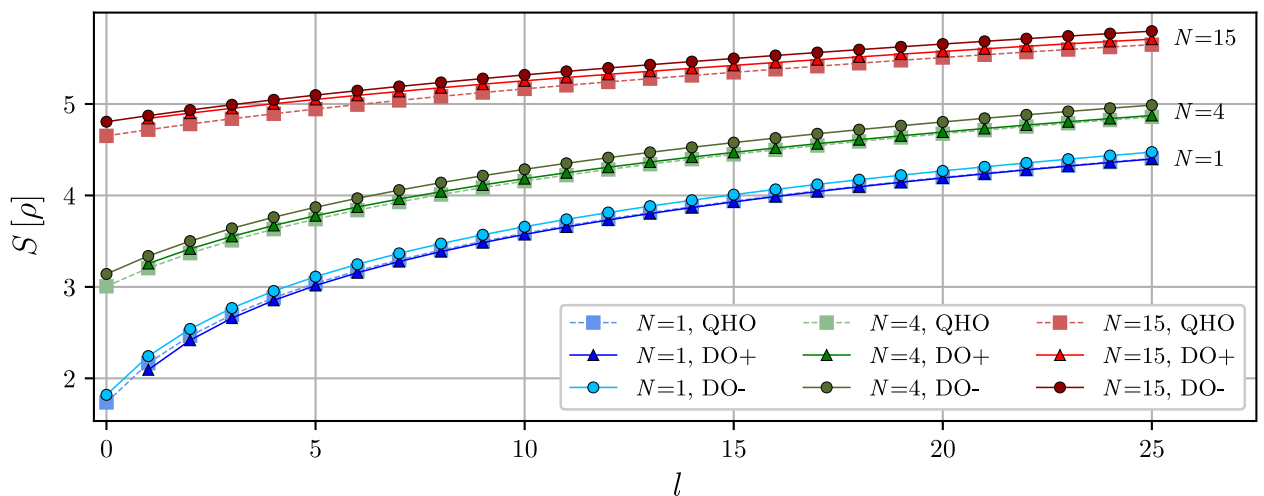

FIG. 4. Shannon entropy $S[\rho]$ as a function of the orbital angular momentum l, for systems DO$\pm$ and QHO with $\omega = 5$. Atomic units (a.u.) are used.

TABLE I. Powers of the fittings $S \sim N^a$ of the Shannon entropy $S[\rho]$ in terms of the radial quantum number N, and the respective correlation coefficients, for oscillators QHO, DO+ and DO− with orbital angular momentum l.

Quantum number	Oscillator QHO		Dirac oscillator DO+		Dirac oscillator DO−	
	Fittings $S \sim N^a$ of Shannon entropy					
l	Power a	Correlation	Power a	Correlation	Power a	Correlation
1	0.292 ± 0.002	0.9996	0.311 ± 0.002	0.9994	0.2894 ± 0.0012	0.9998
3	0.224 ± 0.004	0.9952	0.237 ± 0.004	0.9971	0.224 ± 0.003	0.9970
7	0.163 ± 0.005	0.9877	0.173 ± 0.005	0.9895	0.165 ± 0.004	0.9915
12	0.130 ± 0.005	0.9841	0.137 ± 0.005	0.9851	0.132 ± 0.004	0.9890
20	0.104 ± 0.004	0.9828	0.109 ± 0.004	0.9829	0.107 ± 0.003	0.9887

quantum number within the range $N = 0 - 15$. A noticeable decreasing behavior is observed for all the curves, that is, for systems QHO and DO± with arbitrary l.

Overall, the height of curves are higher as l *is lower*. And, as happened with Shannon entropy, they seem to run along corridors determined by each l value. In all cases, for a given l, the curve of DO− is displayed clearly below the other two, which means that this system has a lower disequilibrium or, in other words, is closer to uniformity. Regarding QHO and DO+, the respective curves are much closer among themselves, andbecome roughly overlapped for large l. These comments are valid for the whole range of N, only with slightly observable separation for large N.

In order to better interpret the variation of $D[\rho]$ with increasing N, let us analyze Fig. 1. In spite of the increasing height of the main maximum (what could be interpreted as departure from uniformity), the region of density values closer to zero enlarges as N increases. For illustration, values out from the narrow strip $\rho(r) < 0.05$ beyond the maximum of DO− are limited roughly to $r = 0.7$ for $N = 8$, while they extend up to $r = 1.3$ for $N = 1$ (thus with a larger region of departure from the lower strip).

On the other hand, the dependence of $D[\rho]$ on the quantum number l is observed in Fig. 6 for different N's. Again, a decreasing monotonicity is systematically displayed in all cases, with similar shapes. Trios of curves are distinguished

accordingly with each fixed value of N, the height of the groups being ordered from above to below for increasing N. As in the previous figure, the curves of the system DO− clearly distinguish from the other two, and these ones (DO+ and QHO) almost overlap among themselves for the whole range of l. Nevertheless, some crossovers are observed, particularly in the steps: $l = 3 - 4$ (for $N = 4$) and $l = 1 - 2$ (for $N = 15$).

Let us now discuss the results obtained, looking for power-like dependences $D \sim N^a$ and $D \sim l^a$. Table II provides the main data corresponding to fittings of D in terms of N:

(1) In the three systems, the negative power a decreases (in absolute value) as l increases. As occurred with the monotonicity of the Shannon entropy, also the monotonic trend (now decreasing) of the disequilibrium $D[\rho]$ with N weakens for larger angular momenta.

(2) For each l, the decreasing powers round similar values, and the monotonic rate attenuates for higher l. Systematically the fitting power of disequilibrium for DO+ implies a faster decrease with N as compared to those of QHO and DO+.

(3) All fittings are notably accurate: most of them exceed 0.99, the others round that value.

(4) As for any log-log regression, the null value of the variable N has not been included.

Regarding the relation $D \sim l^a$, let us make the following observations:
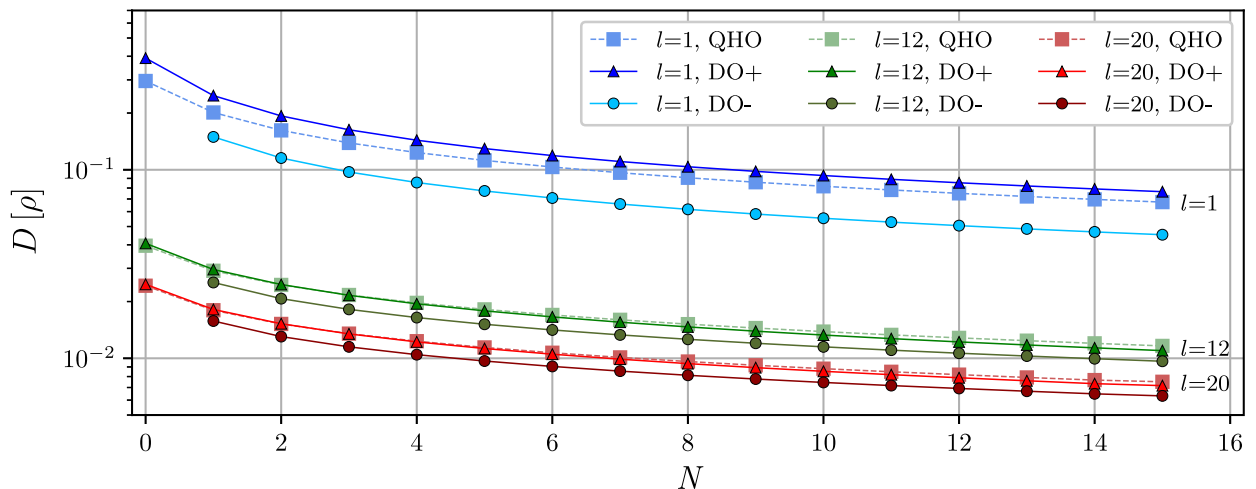

FIG. 5. Disequilibrium $D[\rho]$ as a function of the radial quantum number N, for systems DO± and QHO with $\omega = 5$. Atomic units (a.u.) are used.
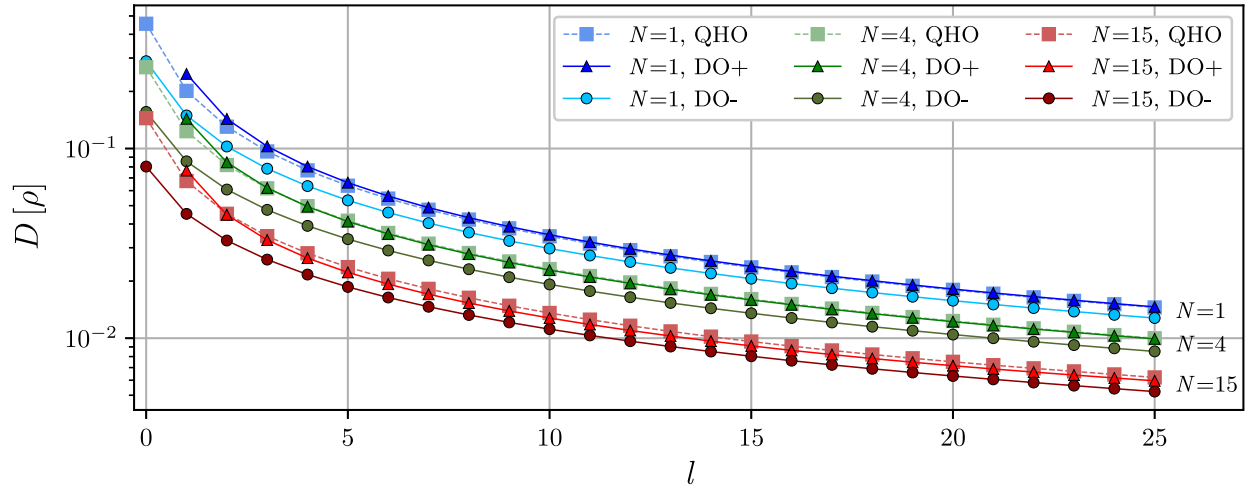
FIG. 6. Disequilibrium $D[\rho]$ as a function of the orbital angular momentum l, for systems DO± and QHO with $\omega = 5$. Atomic units (a.u.) are used.

(1) For the curves $N = 1, 4, 15$ in all systems, fittings are very accurate, with correlation coefficients systematically above 0.99.

(2) All powers belong to the interval $(-0.9, -0.7)$.

(3) Contrary to the heights of curves, there is not a systematic ordering of decreasing rates, neither accordingly to the systems considered nor to the value of N.

D. Fisher information

Let us now analyze the trends of the functional $I[\rho]$, namely the Fisher information given by Eq. (20), when varying the values of each of the quantum numbers N and l. Interestingly, both behaviors are notably different, and the DO+ system distinguishes from the other two in this aspect.

First, an increasing monotonic behavior of $I[\rho]$ as N increases is clearly displayed in all cases. This is shown in Table III, for different values of l (particularly $l = 1, 3, 7, 12, 20$), and for three selected values in Fig. 7. Thus, this provides for the three systems and for the three chosen values of l, a total of 9 curves plotted in Fig. 7. However, not all of them are clearly distinguishable in the figure, due to the notable overlaps of all paths for QHO on one hand, and those of DO− for higher l's, on the other. Even more, the DO− curve for $l = 1$ is only slightly distinguished from the abovementioned other two.

This means that the only system with a noticeable sensitivity to the l value for fixed N is the positive' Dirac one DO+. And oppositely, each of QHO and DO− display roughly identical dependences of $I[\rho]$ in terms of the radial quantum number N for arbitrary values of l. In this sense, it is observed that the higher the orbital angular momentum l, the higher the Fisher information of DO+ is.

The fact that $I[\rho]$ increases monotonically with N is consistent with the density structure. As N increases, the number of oscillations in the density also increases (see Fig. 1), which is reflected by $I[\rho]$ due to its sensitivity to such oscillations.

Furthermore, it is observed that the DO+ and QHO systems display very similar values of Fisher information for $N = 0$ and arbitrary l, because their densities are unimodal, that is, functions with a unique extremum. This is not the case of DO−, since it does not have access to the $N = 0$ state.

The inverse analysis, now keeping fixed l and varying N, is performed on the basis of Fig. 8. As indicated before, different conclusions from those obtained from the study of the dependence on N are derived, particularly for QHO and DO−. In fact, Fisher information for these two systems appears roughly independent of l, maybe excepting the particular case $l = 0$, which deviates from a roughly constant value.

Table IV reveals the closeness of $I[\rho]$ values along the range $l = 1 - 25$, for both QHO and DO−. Only $l = 0$ stands out among the others, and not so much for large N. The data in this table is in agreement with the shapes of curves in Fig. 8

TABLE II. Powers of the fittings $D \sim N^a$ of the disequilibrium in terms of the radial quantum number N, and the respective correlation coefficients, for systems QHO, DO+ and DO− with orbital angular momentum l.

|	Fittings $D \sim N^a$ of disequilibrium					
Quantum number	Oscillator QHO		Dirac oscillator DO+		Dirac oscillator DO−	
l	Power a	Correlation	Power a	Correlation	Power a	Correlation
1	-0.417 ± 0.009	0.9945	-0.444 ± 0.007	0.9970	-0.451 ± 0.007	0.9972
3	-0.393 ± 0.010	0.9923	-0.434 ± 0.009	0.9940	-0.418 ± 0.008	0.9954
7	-0.367 ± 0.010	0.9909	-0.403 ± 0.011	0.9908	-0.385 ± 0.008	0.9941
12	-0.350 ± 0.009	0.9906	-0.379 ± 0.011	0.9897	-0.364 ± 0.008	0.9940
20	-0.335 ± 0.009	0.9913	-0.357 ± 0.010	0.9899	-0.346 ± 0.007	0.9945
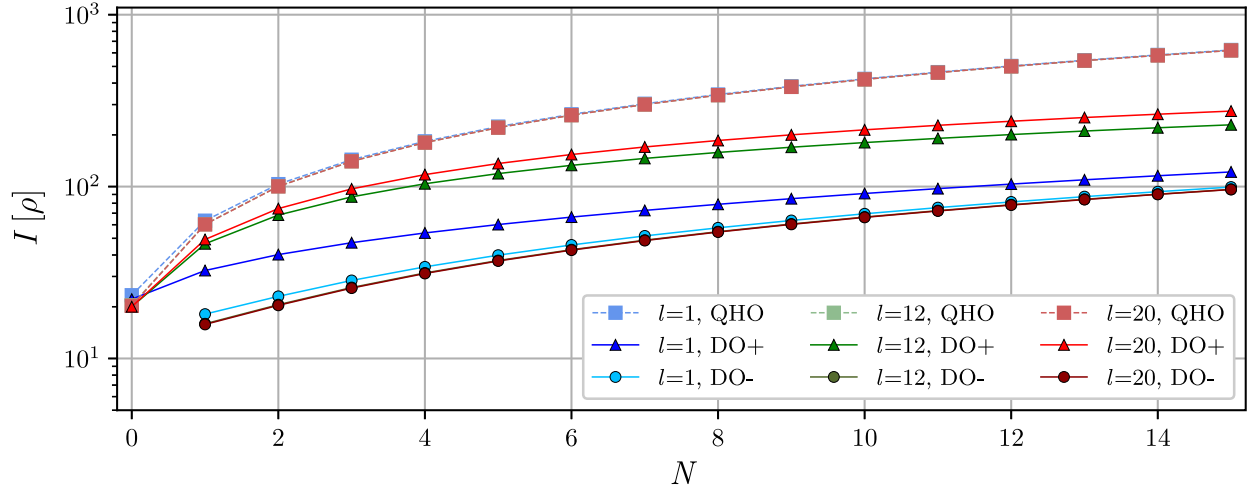
FIG. 7. Fisher information $I[\rho]$ as a function of the radial quantum number N, for systems DO$\pm$ and QHO with $\omega = 5$. Atomic units (a.u.) are used.
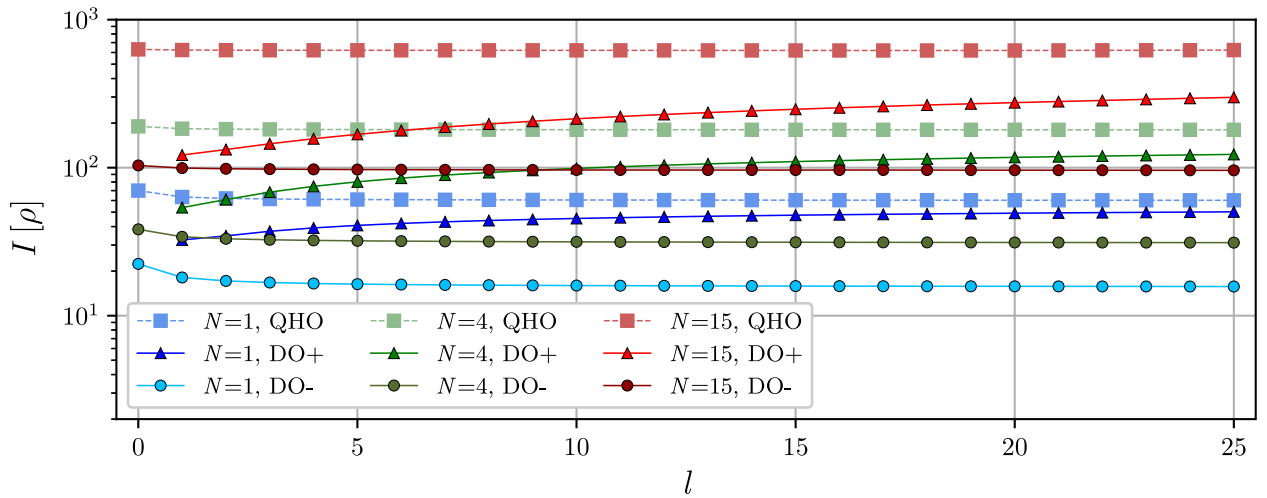

FIG. 8. Fisher information $I[\rho]$ as a function of the orbital angular momentum l, for systems DO$\pm$ and QHO with $\omega = 5$. Atomic units (a.u.) are used.

TABLE III. Powers of the fittings $I \sim N^a$ of the Fisher information in terms of the radial quantum number N, and the respective correlation coefficients, for systems QHO, DO+ and DO$-$ with orbital angular momentum l.

	Fittings $I \sim N^a$ of Fisher information					
Quantum number	Oscillator QHO		Dirac oscillator DO+		Dirac oscillator DO$-$	
l	Power a	Correlation	Power a	Correlation	Power a	Correlation
1	0.864 ± 0.013	0.9970	0.51 ± 0.02	0.9775	0.67 ± 0.03	0.9762
3	0.873 ± 0.012	0.9974	0.512 ± 0.011	0.9940	0.69 ± 0.03	0.9779
7	0.877 ± 0.012	0.9975	0.549 ± 0.003	0.9995	0.70 ± 0.03	0.9783
12	0.878 ± 0.012	0.9976	0.594 ± 0.002	0.9998	0.71 ± 0.03	0.9783
20	0.879 ± 0.012	0.9977	0.643 ± 0.003	0.9998	0.71 ± 0.03	0.9782

TABLE IV. QHO and DO− Fisher information $I[\rho]$ for $N = \{1, 4, 15\}$ as a function of l: range of I values for $l = 1 - 25$, and value for $l = 0$ with the deviation from the top of the range. Atomic units (a.u.) are used.

	Fisher information					
	Oscillator QHO			Dirac oscillator DO−		
Quantum number N	Range for $l = 1-25$	Value for $l = 0$	Deviation (in %)	Range for $l = 1-25$	Value for $l = 0$	Deviation (in %)
1	60.2–63.3	70.0	10.6	15.7–18.1	22.4	23.8
4	180.2–183.3	190.0	3.7	31.2–34.1	38.3	12.3
15	618.9–623.3	630.0	1.1	95.9–99.4	103.5	4.1

for those two systems, appearing as almost straight horizontal lines, only excepting the leftmost point.

On the other hand, the Fisher information of DO+ is clearly an increasing magnitude with l, as observed in Fig. 8. Nevertheless, the rate of increase diminishes quickly for larger l's, particularly for $l \geqslant 10$ becoming $I \sim l^{0.14}$ ($N = 1$), $I \sim l^{0.27}$ ($N = 4$) and $I \sim l^{0.31}$ ($N = 15$), all with correlation coefficients above 0.99.

V. CONCLUSIONS AND OPEN PROBLEMS

A well-known physical system, namely the quantum oscillator, has been studied in this work within an information-theoretical framework. Particular attention has been paid to the spread, uniformity, and fluctuations of the respective probability distributions of the different states, interpreted in terms of meaningful density functionals and their dependences on the characteristic state quantum numbers.

On one hand, the inclusion or not of a relativistic description within the Hamiltonian of the system has been distinguised, and on the other, for the relativistic case, both coupling choices among orbital angular momentum and particle spin. It has been found, in most cases, that the closeness between the Dirac and the Schrödinger solutions strongly depends on the coupling considered, as also occurs with the behavior of the computed functionals for larger/smaller values of the quantum numbers.

For fixed orbital angular momentum, increasing the radial quantum number gives rise, in general, to more delocalized density functions, accordingly to the respective increase of Shannon entropy and decrease of disequilibrium. These magnitudes describes the global behavior, but also the Fisher information displays an increasing behavior, due to the local concentration around the origin of the main peak of the density.

Reverting the role of the quantum numbers, i.e., keeping fixed the radial one, provides similar behaviors regarding the global quantifiers: that is, the global spreading increases as the angular momentum becomes higher. The same comment applies to the Fisher information (local measure) of the DO with positive coupling, while the other two systems (i.e., the other Dirac case and the quantum harmonic oscillator) appear to be roughly independent of the orbital angular momentum.

The main conclusion, from the present work, is that differences between the systems including or not a relativistic description, as quantified by information-theoretical functionals of the respective distributions, are revealed in different ways attending to (i) the specific properties of the measures employed, (ii) the energetic state of the respective systems, and (iii) the spin coupling in the Dirac case. Particularly interesting are the different patterns when considering global or local functionals. This is justified in accordance with the structural characteristics of the radial densities studied.

Future work is considered for this system, in an information-theoretical framework, by considering (i) the total three-dimensional probability distribution, including the angular variables through the spherical harmonics, (ii) complexity measures built up as the product of functionals [30,31,47], and (iii) a comparative study by means of similarity and divergence measures, allowing a direct quantitative comparison among different distributions.

[1] T. M. Cover and J. A. Thomas, *Elements of Information Theory, 2nd ed.* (Wiley-Interscience, New York, 2006).

[2] S. López-Rosa, I. V. Toranzo, P. Sánchez-Moreno, and J. S. Dehesa, Entropy and complexity analysis of hydrogenic Rydberg atoms, J. Math. Phys. **54**, 052109 (2013).

[3] R. O. Esquivel, S. López-Rosa, M. Molina-Espíritu, J. C. Angulo, and J. S. Dehesa, Information-theoretic space from simple atomic and molecular systems to biological and pharmacological molecules, Theor. Chem. Acc. **135**, 253 (2016).

[4] C. Rong, B. Wang, D. Zhao, and S. Liu, Information-theoretic approach in density functional theory and its recent applications to chemical problems, WIREs Comput. Mol. Sci. **10**, e1461 (2020).

[5] J. Antolín, S. López-Rosa, and J. C. Angulo, Rényi complexities and information planes: Atomic structure in conjugated spaces, Chem. Phys. Lett. **474**, 233 (2009).

[6] N. Flores-Gallegos, Informational energy as a measure of electron correlation, Chem. Phys. Lett. **666**, 62 (2016).

[7] R. G. Parr and W. Yang, *Density-Functional Theory of Atoms and Molecules* (Oxford University Press, New York, 1994).

[8] C. E. Shannon, A mathematical theory of communication, Bell Syst. Tech. J. **27**, 379 (1948).

[9] S. E. Massen and C. P. Panos, A link of information entropy and kinetic energy for quantum many-body systems, Phys. Lett. A **280**, 65 (2001).

[10] S. Verdú, Fifty years of Shannon Theory, IEEE Trans. Inf. Theory **44**, 2057 (1998).

[11] A. Lesne, Shannon entropy: A rigorous notion at the crossroads between probability, information theory, dynamical systems and statistical physics, Math. Struct. Comput. Sci. **24**, e240311 (2014).

[12] J. C. Angulo and J. S. Dehesa, Tight rigorous bounds to atomic information entropies, J. Chem. Phys. **97**, 6485 (1992); **98**, 9223 (1993).

[13] J. Pipek and I. Varga, Universal classification scheme for the spatial-localization properties of one-particle states in finite, d-dimensional systems, Phys. Rev. A **46**, 3148 (1992).

[14] J. S. Dehesa, I. V. Toranzo, and D. Puertas-Centeno, Entropic measures of Rydberg-like harmonic states, Int. J. Quantum Chem. **117**, 48 (2017).

[15] R. A. Fisher, Theory of statistical estimation, Math. Proc. Cambridge Philos. Soc. **22**, 700 (1925); Reprinted in Collected Papers of edited by J. H. Bennet (University of Adelaide Press, South Australia, 1972), pp. 15–40.

[16] M. T. Martin, J. Pérez, and A. Plastino, Fisher information and nonlinear dynamics, Physica A **291**, 523 (2001).

[17] S. López-Rosa, R. O. Esquivel, J. C. Angulo, J. Antolín, J. S. Dehesa, and N. Flores-Gallegos, Fisher information study in position and momentum spaces for elementary chemical reactions, J. Chem. Theory Comput. **6**, 145 (2010).

[18] B. R. Frieden, *Science from Fisher Information* (Cambridge University Press, Cambridge, 2004).

[19] T. Yamano, Relative Fisher information for Morse potential and isotropic quantum oscillators, J. Phys. Commun. **2**, 085018 (2018).

[20] S. J. C. Salazar, H. G. Laguna, and R. P. Sagar, Statistical correlation measures from higher-order moments in quantum oscillator systems, Adv. Theory Simul. **4**, 2000322 (2021).

[21] S. J. C. Salazar, H. G. Laguna, and R. P. Sagar, Pairwise and higher-order statistical correlations in excited states of quantum oscillator systems, Eur. Phys. J. Plus **137**, 19 (2022).

[22] S. J. C. Salazar, H. G. Laguna, and R. P. Sagar, Higher-order statistical correlations in three-particle quantum systems with harmonic interactions, Phys. Rev. A **101**, 042105 (2020).

[23] N. Aquino and R. A. Rojas, Accurate calculations of radial expectations values for confined hydrogen-like atoms and isotropic harmonic oscillator, Few Body Syst. **61**, 16 (2020).

[24] N. Aquino and E. Cruz, The 1-dimensional confined harmonic oscillator revisited, Rev. Mex. Fis. **63**, 580 (2017).

[25] H. E. Montgomery Jr., G. Campoy, and N. Aquino, The confined N-dimensional harmonic oscillator revisited, Phys. Scr. **81**, 045010 (2010).

[26] A. Ghosal, N. Mukherjee, and A. K. Roy, Information entropic measures of a quantum harmonic oscillator in symmetric and asymmetric confinement within an impenetrable box, Ann. Phys. **528**, 796 (2016).

[27] N. Mukherjee and A. K. Roy, Information-entropic measures in confined isotropic harmonic oscillator, Adv. Theory Simul. **1**, 1800090 (2018).

[28] D. Nath and A. K. Roy, Average energy and Shannon entropy of a confined harmonic oscillator in a time-dependent moving boundary, J. Math. Chem. **61**, 1491 (2023).

[29] H. G. Laguna and R. P. Sagar, Quantum uncertainties of the confined harmonic oscillator in position, momentum and phase-space, Ann. Phys. **526**, 555 (2014).

[30] P. Maldonado, A. Sarsa, E. Buendía, and F. J. Gálvez, Relativistic effects on complexity indexes in atoms in position and momentum spaces, Phys. Lett. A **374**, 3847 (2010).

[31] P. A. Bouvrie, S. López-Rosa, and J. S. Dehesa, Quantifying dirac hydrogenic effects via complexity measures, Phys. Rev. A **86**, 012507 (2012).

[32] J. Antolín, J. C. Angulo, S. Mulas, and S. López-Rosa, Relativistic global and local divergences in hydrogenic systems: A study in position and momentum spaces, Phys. Rev. A **90**, 042511 (2014).

[33] T. Yamano, Fisher information of radial wavefunctions for relativistic hydrogenic atoms, Chem. Phys. Lett. **731**, 136618 (2019).

[34] O. L. de Lange, Algebraic properties of the Dirac oscillator, J. Phys. A **24**, 667 (1991).

[35] O. L. de Lange and R. E. Raab, *Operator Methods in Quantum Mechanics* (Clarendon Press, Oxford, 1991).

[36] J. Benítez, R. P. Martínez-y-Romero, H. N. Núñez-Yépez, and A. L. Salas-Brito, Solution and hidden supersymmetry of a Dirac oscillator, Phys. Rev. Lett. **64**, 1643 (1990); Erratum: *ibid.* **65**, 2085 (1990).

[37] R. P. Martínez-y-Romero, H. N. Núñez-Yépez, and A. L. Salas-Brito, Relativistic quantum mechanics of a Dirac oscillator, Eur. J. Phys. **16**, 135 (1995).

[38] B. H. Bransden and C. J. Joachain, *Quantum Mechanics*, 2nd ed. (Pearson - Prentice Hall, Englewood Cliffs, New Jersey, 1991).

[39] R. J. Yáñez, W. Van Assche, and J. S. Dehesa, Position and momentum information entropies of the D-dimensional harmonic oscillator and hydrogen atom, Phys. Rev. A **50**, 3065 (1994).

[40] J. Sañudo and R. López-Ruiz, Some features of the statistical complexity, Fisher-Shannon information and Bohr-like orbits in the quantum isotropic harmonic oscillator, J. Phys. A **41**, 265303 (2008).

[41] P. Hohenberg and W. Kohn, Inhomogeneous electron gas, Phys. Rev. **136**, B864 (1964).

[42] C. Arndt, *Information Measures* (Springer, Berlin, 2013).

[43] S. R. Gadre, *In Reviews of Modern Quantum Chemistry: A Celebration in the Contributions of Robert G. Parr, Vol. 1.* (World Scientific, Singapore, 2003).

[44] J. S. Dehesa, S. López-Rosa, and D. Manzano, Entropy and complexity analyses of *d*-dimensional quantum systems, In K. D. Sen, editor, *Statistical Complexities: Applications in Electronic Structures* (Springer, Berlin, 2010).

[45] M. Molina-Espíritu, *Química de la Información: Aspectos clásicos y cuánticos de fenómenos moleculares*, 2015, Ph.D. thesis, Universidad Metropolitanan de Mexico-Iztapalapa.

[46] R. Nalewajski, *Quantum Information Theory of Molecular States* (Nova Biomedical Books, Hauppauge, New York, 2016).

[47] R. López-Ruiz, H. L. Mancini, and X. Calbet, A statistical measure of complexity, Phys. Lett. A **209**, 321 (1995).

[48] R. Carbó, L. Lleyda, and M. Arnau, How similar is a molecule to another? An electron density measure of similarity between two molecular structures, Int. J. Quantum Chem. **17**, 1185 (1980).

[49] O. Onicescu, Theorie de l'information. Energie informationelle, C. R. Acad. Sci. Paris A **263**, 841 (1966).

[50] R. Catalán, J. Garay, and R. López-Ruiz, Features of the extension of a statistical measure of complexity to continuous systems, Phys. Rev. E **66**, 011102 (2002).

[51] J. C. Angulo, J. Antolín, and K. D. Sen, Fisher-shannon plane and statistical complexity of atoms, Phys. Lett. A **372**, 670 (2008).

[52] A. Rényi, *On Measures of Information and Entropy*, Vol. 1 (University of California Press, Oakland, 1961).